Cellular and Molecular Life Sciences (2023) 80:8
https://doi.org/10.1007/s00018-022-04601-x

ORIGINAL ARTICLE

B3galt5 deficiency attenuates hepatocellular carcinoma by suppressing mTOR/p70s6k-mediated glycolysis

Xiaoling Zhang[1,2] · Hao Liu[1,3] · Haidong Wang[1] · Rongjie Zhao[1] · Qian Lu[1] · Yunlong Liu[1,3] · Yicheng Han[1] · LuluRen[1] · Hongming Pan[1] · Weidong Han[1]

Received: 2 November 2021 / Revised: 12 October 2022 / Accepted: 14 October 2022 / Published online: 10 December 2022

Abstract

Hepatocellular carcinoma (HCC) is one of the most common malignancies with high morbidity and mortality. Beta-1,3-galactosyltransferase 5 (b3galt5) plays crucial roles in protein glycosylation, but its function in HCC remains unclear. Here, we investigated the role and underlying mechanism of b3galt5 in HCC. We found that b3galt5 is highly expressed and associated with a poor prognosis in HCC patients. In vitro studies showed that b3galt5 promoted the proliferation and survival of HCC cells. We also demonstrated that b3galt5 deficiency suppressed hepatocarcinogenesis in DEN/TCPOBOP-induced HCC. Further investigation confirmed that b3galt5 promoted aerobic glycolysis in HCC. Mechanistically, b3galt5 promoted glycolysis by activating the mTOR/p70s6k pathway through O-linked glycosylation modification on mTOR. Moreover, p70s6k inhibition reduced the expression of key glycolytic enzymes and the glycolysis rate in b3galt5-overexpressing cells. Our study uncovers a novel mechanism by which b3galt5 mediates glycolysis in HCC and highlights the b3galt5-mTOR/p70s6k axis as a potential target for HCC therapy.

Keywords HCC · B3galt5 · Glycolysis · mTOR · p70s6k · Glycosylation

Introduction

Protein glycosylation is one of the most common and complex modifications and includes N-linked and O-linked glycosylation [1, 2]. It has been reported that protein glycosylation is usually altered in tumor cells, which affects cell adhesion, recognition, invasion, and metastasis [3]. In addition, glycoproteins are commonly used as tumor biomarkers in the clinic, such as alpha-fetoprotein (AFP) and glypican-3 for liver cancer, cancer antigen 125 (CA125) for ovarian cancer, carcinoembryonic antigen (CEA) for colon cancer, prostate-specific antigen (PSA) for prostate cancer, and carbohydrate antigen 19-9 (CA19-9), also known as sialyl-Lewis A (SLA), for gastrointestinal cancer [4].

Glycosylation is catalyzed by glycosyltransferase through the transfer of active glycans to specific receptors with several linkages [5]. The β-1,3-galactosyltransferase family, one of the major types of glycosyltransferase families, transfers active UDP-galactose, UDP-N-acetylglucosamine or UDP-N-acetylgalactosamine to acceptor sugars in a β-1,3 linkage. At present, there are seven members in the b3galt family (namely, b3galt1–7). B3galt5 is directly responsible for the synthesis of Galβ1-3GlcNAcβ (type 1 chain) and other N-glycans with the GlcNAc β1-3 Gal β1-4 GlcNAc β1-R side chains present in CEA [6]. B3galt5 also exhibits a preference for the O-linked *core3* structure (GlcNAc β1-3 GalNAc) [7]. And the *core3* structure is important in the O-linked glycosylation. It has been reported that b3galt5 contributes to the progression of diverse cancers. High expression of b3galt5 is associated with poor clinical outcomes, including shorter overall survival (OS) and

Xiaoling Zhang and Hao Liu have contributed equally.

✉ Hongming Pan
panhongming@zju.edu.cn

✉ Weidong Han
hanwd@zju.edu.cn

1 Department of Medical Oncology, Sir Run Run Shaw Hospital, School of Medicine, Zhejiang University, 3# East Qingchun Road, Hangzhou 310016, Zhejiang, China

2 Department of Medical Oncology, Hangzhou First People's Hospital, School of Medicine, Zhejiang University, Hangzhou, Zhejiang, China

3 Laboratory of Cancer Biology, Institute of Clinical Science, Sir Run Run Shaw Hospital, School of Medicine, Zhejiang University, Hangzhou, Zhejiang, China

recurrence-free survival (RFS) in breast cancer patients, especially early-stage patients [8]. In addition, b3galt5 promotes the proliferation, migration, invasion and epithelial-mesenchymal transition (EMT) of breast cancer by upregulating the expression of β-catenin and EMT activator zinc finger E-box binding homeobox 1 (ZEB1) [8]. Chuang et al. reported that knockdown of b3galt5 disrupted the focal adhesion kinase (FAK)/caveolin-1/AKT/receptor-interacting protein kinase (RIP) complex and caused the dissociation of RIP from the complex, thus inducing breast cancer apoptosis [9]. B3galt5 expression promotes the production of CA19-9, which results in rapid and severe pancreatitis and aggressive pancreatic cancer in cooperation with the $Kras^{G12D}$ oncogene [10]. B3galt5 also functions as a tumor marker for the diagnosis of gynecological cancers. For instance, the b3galt4/b3galt5-positive rates in the sera from ovarian cancer and uterine cervical cancer patients were comparable with the CA125 and SCC antigen-positive rates for these cancers [11].

Primary liver cancer (hepatocellular carcinoma, HCC), ranking second in malignant tumor-associated deaths, is one of the most common malignant tumors in China with a rising incidence [12]. The molecular mechanisms of HCC are very complex. Accumulating evidence indicates that metabolic alterations are deeply involved in HCC pathogenesis [13, 14]. Metabolic reprogramming from oxidative phosphorylation (OXPHOS) to glycolysis was found in very early stages of hepatocarcinogenesis and was maintained in advanced HCC, suggesting that it is an important event in the progression of HCC development [15]. Studies have shown that liver cancer cells exploit glycolysis to fulfill energetic and biosynthetic needs of rapid proliferation and survival [16]. Multiple signaling pathways, such as mTOR/p70s6k, c-Myc, and p53, are important regulators of glycolysis in cancer [17, 18] and increase the expression of key glycolytic enzymes, including hexokinase-2 (HK2), pyruvate kinase M2 (PKM2), and lactate dehydrogenase A (LDHA) [19].

High expression of b3galt5 is associated with advanced Tumor-Node-Metastasis stage, metastasis, poor survival and a high recurrence rate of HCC [20]. It was reported that b3galt5 was upregulated in metastatic HCC cell lines [21]. Moreover, hepatitis B virus X protein (HBx) induced the expression of b3galt5, which was associated with higher expression of SLA, thereby promoting liver cancer metastasis by interacting with endothelial cells [22]. However, the molecular mechanisms underlying b3galt5-mediated glycosylation in HCC have not been elaborated. In this study, we demonstrated that b3galt5 was upregulated in HCC and that its deficiency inhibited liver tumorigenesis in vivo and in vitro. Mechanistically, b3galt5 activated the mTOR/p70s6k pathway through O-linked glycosylation modification on mTOR to enhance glycolysis in HCC. Thus, our study reveals an important role and novel mechanism of b3galt5-mediated glycosylation in promoting the progression of HCC, which indicates a potential target for the diagnosis and treatment of HCC.

Materials and methods

HCC patient specimens

Tissue microarrays (TMAs), which contained 90 dots corresponding to HCC tissues and matching normal tissues with complete clinical pathological information, were purchased from Shanghai Outdo Biotech Co., Ltd. (Shanghai, China). Written informed consent was obtained from all enrolled subjects according to the Declaration of Helsinki. Three hundred and seven liver tumor tissues and adjacent nontumorous tissues were obtained from Sir Run Run Shaw Hospital. This study was approved by the Ethics Committee of Sir Run Run Shaw Hospital, Zhejiang University (20201113-30).

Cell lines and culture

The human HCC cell lines HUH7, PLC/PRF/5, HCCLM3, and HLE and the normal hepatocyte cell line LO2 were purchased from the Shanghai Institute of Biological Science, Chinese Academy of Science (Shanghai, China). All cells were cultured in DMEM (high glucose) with 10% fetal bovine serum (FBS, Gibco).

Mice

The $b3galt5^{-/-}$ mice were a generous gift from Prof. Jinhan He (Department of Pharmacy, West China Hospital of Sichuan University). C57BL6/J mice were purchased from Shanghai Laboratory Animal Center (SLAC, Shanghai, China). All mice were bred and maintained in a specific pathogen-free facility at Zhejiang University Animal Center. All animal experiments were performed in accordance with the protocols approved by the Animal Care and Use Committee of Zhejiang University.

DEN/TCPOBOP-induced HCC

Two-week-old male C57BL6/J mice were intraperitoneally injected with one dose of N-nitrosodiethylamine (DEN, #N0258, Sigma, USA) at 25 mg/kg. At 4 weeks, the mice received biweekly intraperitoneal injections of 2.5 mg/kg TCPOBOP (#T1443, Sigma, USA) 8 times. Meanwhile, the mice were fed a high-fat diet (HFD) (#D112252, Research Diets, USA). Liver nodule formation was observed by B-ultrasound. At 18 weeks, mice were injected with AAV8 vectors carrying b3galt5 shRNA or scramble shRNA (2×10^{12} viral genomes/kg, Genomeditech, China) via the

tail vein (referred to as shb3 AAV8 and shNC AAV8, respectively); 24 weeks later, all mice were sacrificed, and livers were excised. The tumor number, tumor size, liver weight, and body weight were measured.

For b3galt5 knockout mice, HCC was induced by injection with DEN (25 mg/kg, i.p.) at day 14 followed by biweekly injections of TCPOBOP (2.5 mg/kg, i.p.) 5 times starting at 4 weeks. Mice were sacrificed at 20 weeks.

siRNA transfection

The target cells were cultured at 80% confluence and transfected with human b3galt5-specific siRNA, p70s6k-specific siRNA, or a negative siRNA control using RNAimax (Thermo Fisher Scientific, MA, USA) according to the manufacturer's protocol. The efficiency of transfection was detected by western blotting. B3galt5 siRNA (GGG CATAGAATGGGTCCATTT, GCAAGTGGTTTGTCA GTAATT), p70s6k siRNA (GACGGGGTCCTCAAATGT A, CCAAGGTCATGTGAAACTA), and scramble siRNA (GATCATACGTGCGATCAGA) were purchased from RiboBio (Guangzhou, China).

Construction of stable overexpressing cell lines

Lentiviruses expressing empty vector (pGMLV-CMV-MCS-EF1-ZsGreen1-T2A-puro) and HA-b3galt5 were purchased from Genomeditech (Shanghai, China). To establish stable b3galt5-overexpressing cells, the target cells were infected with 3×10^6 transducing units (TU)/well. The infected cells were selected with 2.5 μg/mL puromycin for 2 weeks. The efficiency of overexpression was determined by western blotting.

Glycosidase treatment

Samples were heated at 100 °C for denaturation. The denatured proteins were chilled on ice, and then centrifuged. Afterward, peptide-*N*-glycosidase F (PNGase F, New England Biolabs) or O-glycosidase (New England Biolabs) was added to the denatured proteins, and incubation at 37 °C for 1 h was performed according to the manufacturer's instructions.

Coimmunoprecipitation (Co-IP) assay

Total proteins were extracted from target cells by NP40 buffer (Meilunbio, Dalian, China) according to the manufacturer's instructions. Ricinus communis agglutinin (RCA)-I/II lectin (Vector laboratories, CA, USA) antibody, which is a plant-derived protein that binds specifically but non-immunologically to galactose or N-acetylgalactosamine residues of glycoconjugates [23], protein A/G agarose beads and protein lysate were incubated together at 4 °C overnight. The beads were washed 5 times with NP40 buffer and collected by centrifugation at 15,000 rpm. SDS (2×) was added to the beads, and the beads were subjected to western blotting.

Extracellular acidification rate (ECAR) and oxygen consumption rate (OCR) assays

The ECAR and OCR were analyzed using a Seahorse XFe 96 extracellular flux analyzer (Agilent, CA, USA). Briefly, 1.5×10^4 cells were plated in a Seahorse XF 96 cell culture microplate. For ECAR, 10 mM glucose, 1 μM oligomycin and 50 mM glycolytic inhibitor 2-DG were sequentially injected into each well at the indicated time points. For OCR, 1 μM oligomycin, 1 μM p-trifluoromethoxy carbonyl cyanide phenylhydrazone (FCCP) and 0.5 μM mitochondrial complex III inhibitor rotenone/antimycin A (Rote/AA) were sequentially injected into the wells. Data were analyzed by Seahorse XF-96 wave software. The ECAR and OCR were normalized to cell number.

Lactate content measurement

Mouse serum and cell supernatants were collected at the indicated times for lactate content measurement using a lactate colorimetric assay kit (Jiancheng, Nanjing, China) following the manufacturer's protocol.

RNA extraction and quantitative RT-PCR analysis

RNA was extracted from liver tissues using TRIzol reagent (Thermo Fisher Scientific, MA, USA), and mRNA was reverse transcribed into cDNA with the HiScript III RT SuperMix for qPCR Kit (Vazyme, Beijing, China). cDNA was quantified with the Ultra SYBR One Step qPCR Kit (CWBIO, Beijing, China). B2M was used as an endogenous control. The primer sequences were as follows: mouse *b3galt5* forward CATGCCCTTCATCCACCTGT, reverse ATACCCAGTTGGGGATCGAC; mouse *B2M* forward TCGCGCTACTCTCTCTTTCT, reverse TGTCGGATG GATGAAACCCA.

Immunohistochemistry (IHC) staining and IHC score assay

A tissue microarray containing 90 HCC patients was obtained from Shanghai Outdo Biotech Co., Ltd. (Shanghai, China). The IHC assay was performed as previously described [24]. Anti-b3galt5 antibody (#45804, SAB, CA, USA) and anti-phospho-p70s6k (#RT1456, HuaBio, Hangzhou, China) antibodies were used. The immunoreactive score, judged by two independent pathologists who were blinded to the histopathological features and patient data of

the samples, was determined by the staining index (SI). The IHC score of mice liver cancer tissues was calculated by multiplying the stain intensity (0 = negative, 1 = canary yellow, 2 = claybank, and 3 = brown) by the percentage of positive cells score (1 = less than 25%, 2 = 25–50%, 3 = 51–75%, and 4 = more than 75%).

Immunofluorescence staining

Cells were fixed with 4% paraformaldehyde, permeabilized with 0.5% Triton X-100, and washed 3 times with PBST buffer. Then, the samples were blocked with 3% BSA for 1 h at room temperature, successively incubated overnight with antibodies against Ricinus Communis Agglutinin (RCAI&II) (Vector Laboratories, AS-2084-1), phospho-mTOR (CST, #5536) at 4 ℃. After washed 3 times with PBST buffer, cells were further incubated with Alexa Fluor-labeled secondary antibodies (IFKine™ Red Donkey anti-Rabbit IgG (Abbkine, A24421), Donkey anti Goat IgG Highly adsorbed secondary antibody, Aleax Fluro™ plus 405(Invitrogen, A48259), IFKine™ Green Donkey anti-Goat IgG (Abbkine, A24231)). Nuclei were stained with 4',6-diamidino-2-phenylindole (DAPI) at room temperature for 30 min. The images were captured and analyzed by using a Leica sp8 laser scanning confocal microscope (Leica, Germany).

Statistical analysis

Data are presented as the mean ± SEM of the indicated number of litters. mRNA expression, tumor volume, tumor number and tumor weight/body weight ratio were analyzed using two-tailed unpaired Student's *t* test. The analysis was performed with GraphPad Prism 7 software. The correlation analysis was measured by Pearson analysis. $P < 0.05$ was considered statistically significant.

All other methods are described in the supplementary materials.

Results

B3galt5 is upregulated in HCC patients

We first examined the mRNA and protein expression of b3galt5 in tumor tissues and adjacent normal tissues in HCC patients using RNA-seq and western blotting. The mRNA level of b3galt5 in HCC tissues was significantly increased compared with that in paired normal tissues (Fig. S1A). Analysis of b3galt5 expression in HCC from the Gene Expression Omnibus dataset GSE1898 also confirmed a consistently higher b3galt5 level in tumor tissues (Fig. S1B). Furthermore, we determined the protein level of b3galt5 in HCC samples, which was also dramatically elevated compared with the adjacent normal tissues, indicating the upregulation of b3galt5 in HCC tissues (Fig. S1C). Importantly, Kaplan–Meier survival analysis revealed that HCC patients with high b3galt5 expression ($n = 259$) were associated with poor overall survival, while low expression ($n = 111$) prolonged overall survival (Fig. S1D). Overall, these results indicated that b3galt5 might act as a tumor promoter in HCC.

B3galt5 promotes proliferation and inhibits apoptosis in HCC cells

To explore the biological functions of b3galt5 in HCC cells, we first screened two cell lines, HLE and HCCLM3, with high b3galt5 expression profiles from a series of HCC cell lines (Fig. S2A). Then, we silenced b3galt5 in HLE and HCCLM3 cells using specific siRNA. Intriguingly, the proliferation of these two cell lines was significantly inhibited after b3galt5 knockdown, as determined by the CCK-8 assay (Fig. S2B). The apoptotic rates of HLE and HCCLM3 cells with b3galt5 silencing were 12.83% ± 0.06% and 16.87% ± 0.22%, respectively, compared with rates of 7.60% ± 0.10% and 12.27% ± 1.83% in siRNA control cells, respectively (Fig. S2C and D). Moreover, b3galt5 knockdown disrupted cell cycle progression and induced G0/G1-phase arrest (Fig. S2E and F). Taken together, these results indicated that b3galt5 promoted proliferation and inhibited apoptosis in HCC cells.

B3galt5 deficiency attenuates DEN/TCPOBOP-induced hepatocarcinogenesis

To further investigate the role of b3galt5 in liver tumorigenesis, we attempted to silence b3galt5 in a DEN/TCPOBOP-induced mouse HCC model. C57BL/6 male mice were treated with DEN at day 14 followed by biweekly injections of TCPOBOP for 8 times starting at 4 weeks postpartum. Then, mice were given tail vein injections of shNC AAV8 or shb3 AAV8 at 18 weeks old (Fig. S3A). As expected, b3galt5 expression was markedly decreased in shb3 AAV8-treated mice (Fig. S3B and C), and the incidence of liver cancer in shb3 AAV8 mice was lower than that in shNC AAV8 mice (Fig. S3D). Histopathological analysis of livers showed that there were more fat deposits and more severe dysplasia in shNC AAV8 mice than in shb3 AAV8 mice (Fig. S3E). Quantitative analysis showed that shb3 AAV8 mice had an ~ 60% decrease in tumor number (Fig. S3F). In addition, although the difference was not statistically significant, the tumor volume showed a decreasing trend in shb3 AAV8 mice (Fig. S3G). The liver weight/body weight ratio was similar in both groups of mice (Fig. S3H). We further assessed the IHC scores of PCNA and cleaved caspase-3 in

shNC AAV8 and shb3 AAV8 mice, which were 5.14 ± 1.10 vs 1.43 ± 0.78 and 2 ± 0 vs 7.83 ± 1.93, respectively, indicating massive remission of proliferation-positive cells and induction of apoptosis in the livers after b3galt5 silencing (Fig. S3I). In addition, hepatic fibrosis was markedly alleviated in shb3 AAV8 mice with b3galt5 deficiency, as determined by α-smooth muscle actin (α-SMA) staining (Fig. S3I).

Furthermore, we investigated liver tumorigenesis in b3galt5$^{-/-}$ (KO) and wild-type (WT) mice under DEN/TCPOBOP challenge (Fig. 1A). Mice were sacrificed, and whole livers were collected and analyzed 18 weeks after DEN injection. As expected, the protein and mRNA level of b3galt5 were effectively decreased in KO mice (Fig. 1B–D). Notably, KO mice developed fewer tumors in the liver than WT mice (Fig. 1E). The KO livers exhibited smaller neoplastic lesions and attenuated cirrhosis compared with control littermates, as shown by H&E staining (Fig. 1F). Quantitative analysis revealed that the number of tumor nodules in KO mice was only 3.07 ± 0.50 per liver, which was significantly lower than that in WT mice (12.14 ± 2.83 per liver, Fig. 1G). The tumor volume of KO mice was also markedly reduced compared to that of WT mice (30.33 ± 8.65 vs 131.9 ± 43.58 mm^3, respectively) (Fig. 1H), accompanied by an ~ 20% reduction in the liver/body weight ratio (Fig. 1I). In addition, histopathological analysis demonstrated markedly inhibited proliferation, a significant induction of apoptosis, and attenuated hepatic fibrosis in the livers of KO mice compared to WT mice (Fig. 1J).

Collectively, these results revealed that b3galt5 deficiency attenuated DEN/TCPOBOP-induced HCC in mice.

B3galt5 promotes glycolysis in HCC

To investigate the underlying molecular mechanism of the tumorigenic effect of b3galt5, we performed metabolomics analysis of liver cancer cells from shb3 AAV8 and shNC AAV8 treated mice. The results revealed that the metabolites were significantly changed when b3galt5 was knocked down (Fig. S4A). Kyoto Encyclopedia of Gene and Genomes (KEGG) enrichment analysis identified that multiple carbohydrate metabolism signaling pathways were enriched, including pyruvate metabolism, pentose and glucuronate interconversion, amino sugar and nucleotide sugar metabolism and OXPHOS (Fig. S4B). Next, we performed proteomic sequencing of liver cancer cells from shb3 AAV8- and shNC AAV8-treated mice. A number of key proteins closely associated with OXPHOS, including Cox7a2l [25], Ndufaf3 [26], Cmc1 [27] and Sdhaf4 [28], were significantly upregulated upon b3galt5 knockdown (Fig. S4C). To further explore the function of the b3galt5-regulated proteins, we conducted KEGG enrichment analysis. Our results showed that proteins involved in amino nucleic acid sugar metabolism, glycolysis and gluconeogenesis, and OXPHOS were markedly enriched in b3galt5 knockdown mice (Fig. S4D), suggesting the potential roles of b3galt5 in glucose metabolism.

Inspired by metabolomics analysis and proteomic sequencing, we then examined whether b3galt5 regulated glycolysis in HCC. Compared with control mice, knockout of b3galt5 resulted in a significant decrease in key glycolytic enzymes, including HK2, 6-phosphofructo-2-kinase/fructose-2,6-bisphosphatase 3 (PFKFB3) and LDHA (Fig. 2A). Immunohistochemical staining also confirmed that the expression of LDHA, HK2, and PFKFB3 was decreased in the livers of KO mice (Fig. S5A-C). Additionally, ablation of b3galt5 led to a significant reduction in lactate production and decreased lactate dehydrogenase, hexokinase, and phosphofructokinase activity in the serum of KO mice (Fig. 2B–E). It should be noted that the absence of b3galt5 did not lead to s obvious changes in total pyruvate kinase activity (Fig. 2F), which might be because pyruvate kinase has a variety of isoenzymes, while pyruvate kinase M2 is the main form expressed in liver tissue [29].

In HCCLM3 and HLE cells, silencing b3galt5 likewise decreased the expression of several key glycolytic enzymes, such as HK2, PFKFB3, LDHA and pyruvate dehydrogenase kinase 1 (PDK1) (Fig. 2G). Conversely, overexpression of b3galt5 in LO2 and HUH7 cells increased the expression of these glycolytic enzymes (Fig. 2H). Moreover, b3galt5 knockdown significantly reduced lactate production, while b3galt5 overexpression had the opposite effect (Fig. 2I). Accordingly, we observed an obviously increased rate of ECAR, as indicated by the increased glycolysis rate and glycolysis capacity in b3galt5-overexpressing cells (Fig. 2J, K). Knockdown of b3galt5 in HCCLM3 and HLE cells led to opposing effects (Fig. 2L, M). In addition, we also detected the OCR in HCC cells. As expected, knockdown of b3galt5 in HCCLM3 and HLE cells led to a significant increase in the OCR. In particular, the maximal respiration in HLE cells increased from 42.1 ± 3.8 to 49.1 ± 6.2 pmol/min, and in HCCLM3 cells, it increased from 31.0 ± 3.9 to 64.7 ± 5.5 pmol/min (Fig. 3A–C). In contrast, a significant reduction in maximal respiration in LO2 and PLC/PRF5 cells was observed after b3galt5 overexpression (Fig. 3D–F). All these compelling results suggested that b3galt5 promoted glycolysis in HCC.

B3galt5 promotes glycolysis in HCC via the mTOR pathway

The mTOR pathway is one of the main signaling pathways that regulates glycolysis. To clarify its role in the promotion of glycolysis by b3galt5, we detected the total and phosphorylated protein levels of mTOR and its downstream target, p70s6k. Immunoblot analysis showed that

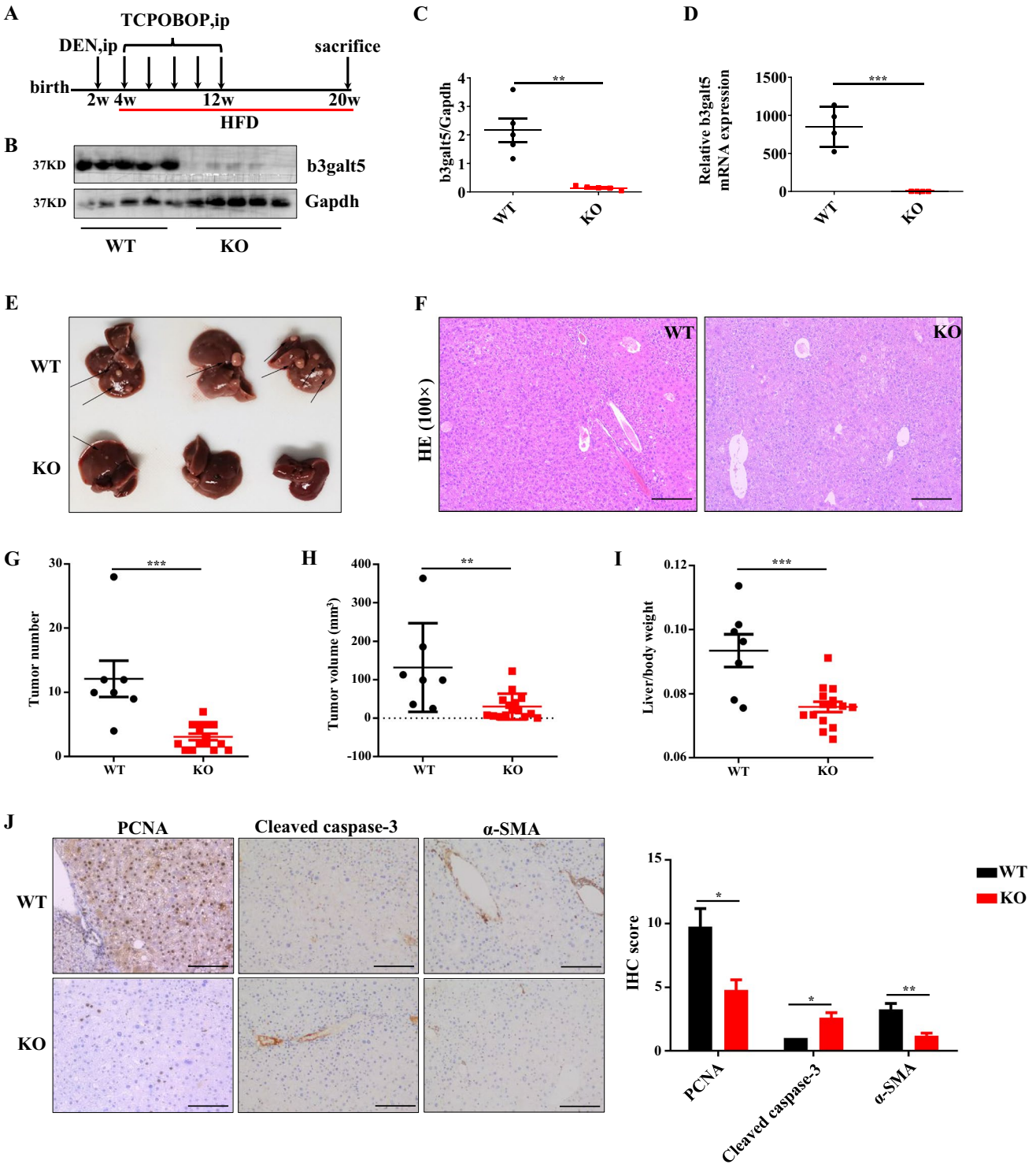

Fig. 1 B3galt5 deletion prevents DEN/TCPOBOP-induced hepatocarcinogenesis in mice. (**A**) Schematic representation of the experimental design. (**B**, **C**) Western blotting and quantitative analysis of b3galt5 expression in liver tissues measured by Image J software ($n=5$). (**D**) Quantitative analysis of b3galt5 mRNA expression in liver tissues measured by qRT-PCR. (**E**) Representative images of liver tumors are shown. Black arrows indicate the liver tumors. (**F**) Representative HE-stained sections are shown. Magnification, × 100. The number of tumors per liver (**G**), tumor volume (**H**), and liver/body weight (**I**) were measured. Data represent the mean ± SEM (WT = 7, KO = 15). Statistical differences were determined by a two-tailed unpaired *t* test, $^{**}p<0.01$, $^{***}p<0.001$. (**J**) IHC staining and score of PCNA, cleaved caspase-3, and α-SMA in WT and KO liver tissues of the DEN/TCPOBOP-induced mice (WT = 4, KO = 5). The IHC score was calculated by multiplying the stain intensity (0 = negative, 1 = canary yellow, 2 = claybank, and 3 = brown) by the percentage of positive cells score (1 = less than 25%, 2 = 25–50%, 3 = 51–75%, and 4 = more than 75%). Magnification, × 200

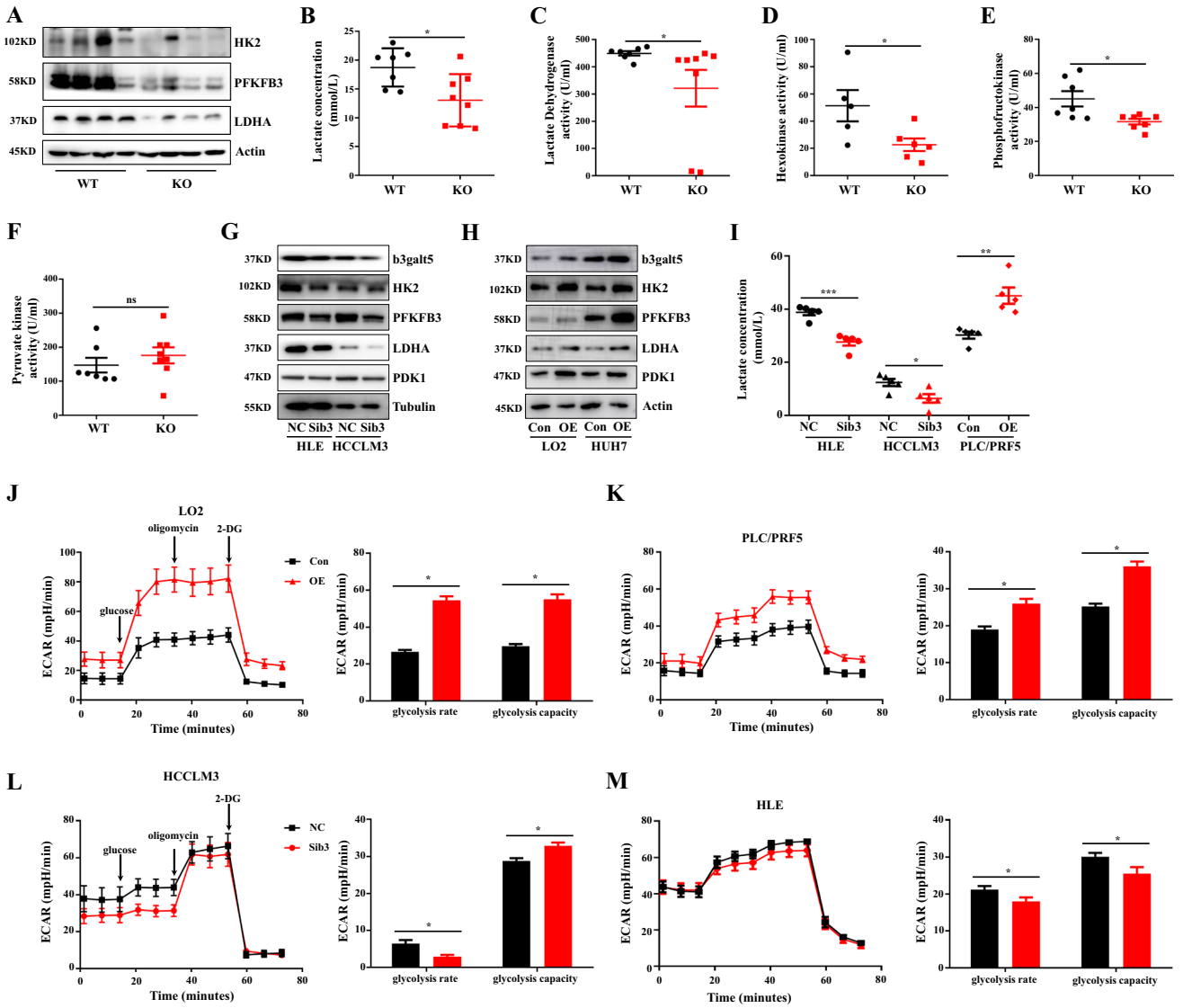

Fig. 2 B3galt5 deficiency inhibits glycolysis in HCC. (**A**) Immunoblot analysis of HK2, PFKFB3, and LDHA from liver cancer extracts. Representative immunoblots are shown of four individual mice per group. Measurements of lactate production (**B**) and lactate dehydrogenase activity (**C**) in mouse serum (WT = 7, KO = 8). (**D**) Measurements of hexokinase activity in mouse serum (WT = 5, KO = 6). (**E**) Measurements of phosphofructokinase activity in mouse serum (WT = 7, KO = 7). (**F**) Measurements of pyruvate kinase activity in mouse serum (WT = 7, KO = 8). The expression of key glycolytic enzymes in the indicated HCC cell lines with either b3galt5 knockdown or control siRNA (**G**), with either b3galt5 overexpression or control vector (**H**) detected by western blotting. (**I**) Measurements of lactate production in the supernatant of HCC cell lines with b3galt5 knockdown or overexpression ($n = 5$). (**J**, **K**) Analysis of the extracellular acidification rate (ECAR) in LO2 and PLC/PRF5 cells with b3galt5 overexpression or control vector using the Seahorse XFe 96 Analyzer. (**L**, **M**) Analysis of the ECAR in HCCLM3 and HLE cells with b3galt5 knockdown or control siRNA using the Seahorse XFe 96 Analyzer. * $p < 0.05$, ** $p < 0.01$, *** $p < 0.001$

both phosphorylated and total protein levels of mTOR, as well as p70s6k, were downregulated in b3galt5-KO liver cells (Fig. 4A). Consistent results could also be observed in HLE and HCCLM3 cells (Fig. 4B). Conversely, in b3galt5-overexpressing LO2 and HUH7 cells, total and phosphorylated mTOR and p70s6k levels were accordingly upregulated (Fig. 4C). As expected, these changes were in line with the expression of key glycolytic enzymes. To further verify the clinical correlation between b3galt5 and p-p70s6k, we performed immunohistochemistry staining in a 90-dot tissue microarray (Fig. S6A). Encouragingly, b3galt5 expression was positively correlated with p-p70s6k in HCC samples ($r = 0.32$, $p = 0.0021$) (Fig. S6B).

Then, we examined whether activation of mTOR mediated the effects of b3galt5 on glycolysis. For this purpose, we treated HCC cells with a p70s6k activator or inhibitor

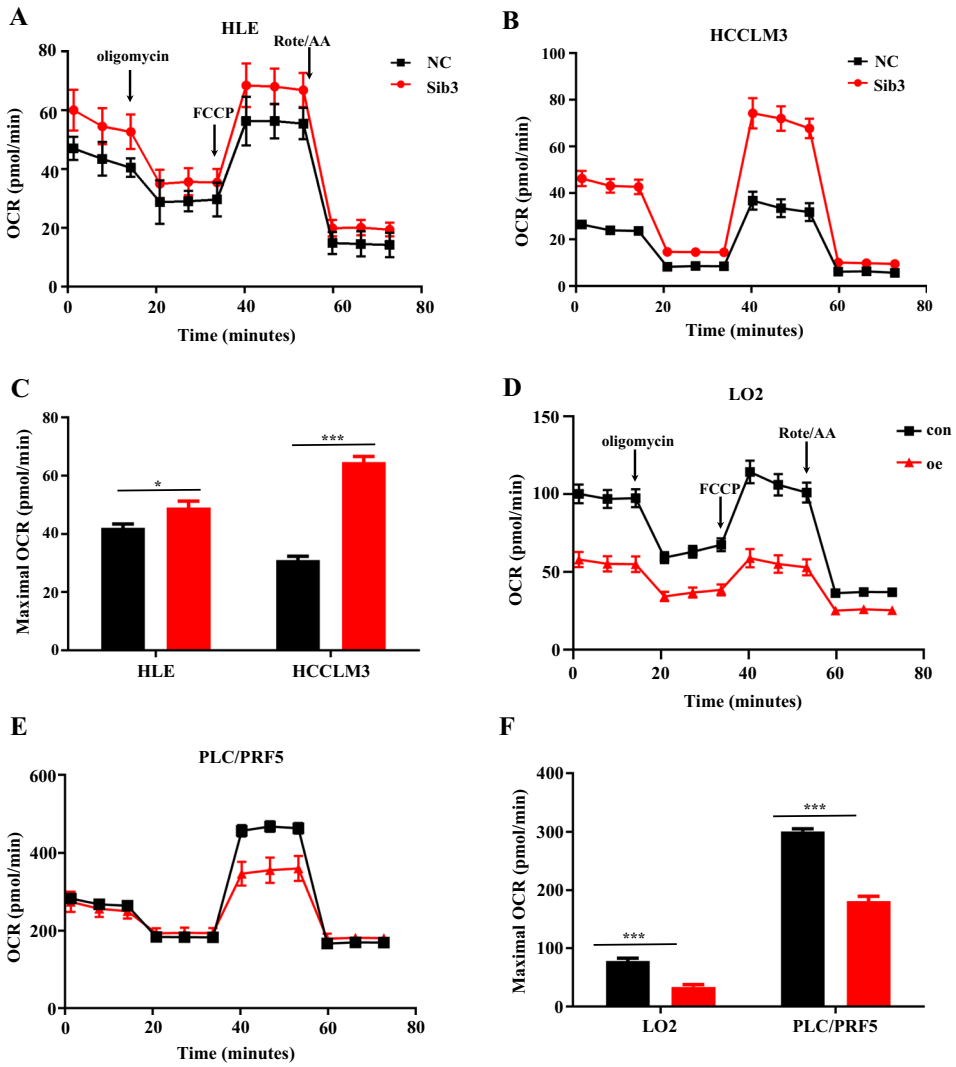

Fig. 3 B3galt5 reduces the oxygen consumption rate in HCC cells. (**A**, **B**) Analysis of the OCR in HLE and HCCLM3 cells with b3galt5 knockdown or control siRNA using the Seahorse XFe 96 Analyzer. (**C**) The maximal respiration of HLE and HCCLM3 cells was analyzed by WAVE software. (**D**, **E**) Analysis of the OCR in LO2 and PLC/PRF5 cells with b3galt5 overexpression or control vector using the Seahorse XFe 96 Analyzer. (**F**) The maximal respiration was calculated by WAVE software. $^{*}p < 0.05$, $^{***}p < 0.001$

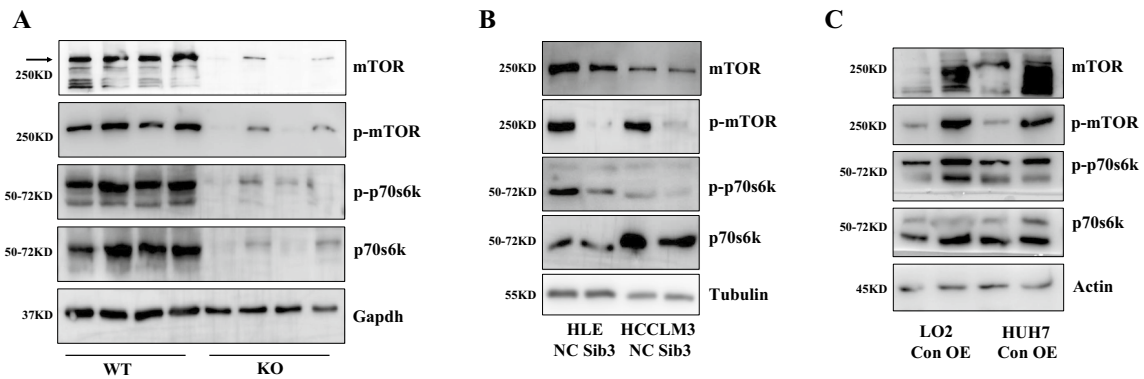

Fig. 4 B3galt5 activates the mTOR pathway. (**A**) Immunoblot analysis of the phosphorylation of mTOR and p70s6k in liver extracts. The phosphorylation of mTOR and p70s6k in the indicated HCC cell lines with either b3galt5 knockdown or control siRNA (**B**) and with either b3galt5 overexpression or control vector (**C**) detected by western blotting

in combination with b3galt5. The results indicated that the expression of key glycolytic enzymes, including HK2, LDHA, PFKFB3, and PKM2, in b3galt5-silenced HLE cells could partially be rescued by 3BDO, an activator of

p70s6k (Fig. 5A). Conversely, the inhibition of p70s6k by PF-4708671 reduced the levels of these key glycolytic enzymes in b3galt5-overexpressing LO2 and PLC/PRF5 cells (Fig. 5B, C). To further confirm the role of p70s6k in b3galt5-mediated glycolysis, we carried out live monitoring using a Seahorse XF Extracellular-Flux Analyzer for ECAR. Knockdown of p70s6k markedly inhibited the glycolysis rate and glycolysis capacity (Fig. 5D–F). Overexpression of p70s6k in b3galt5 knockdown cells rescued the glycolysis rate and glycolysis capacity (Fig. 5G, H).

Collectively, these results illustrated that b3galt5 promoted glycolysis by activating the mTOR/p70s6k pathway.

B3galt5 regulates the O-linked glycosylation of mTOR

It has been reported that glycosylation mediates protein stability, function and transport. We therefore investigated whether the activation of mTOR is regulated by glycosylation. RCA-lectin is a reagent that is generally used to identify the galactose or N-acetylgalactosamine residues of glycoconjugates [30]. Thus, we traced the galactose transferring mediated by b3galt5 in the elongation of glycoconjugates. Immunoblot analysis revealed that b3galt5 knockdown significantly blocked the glycosylation modification of

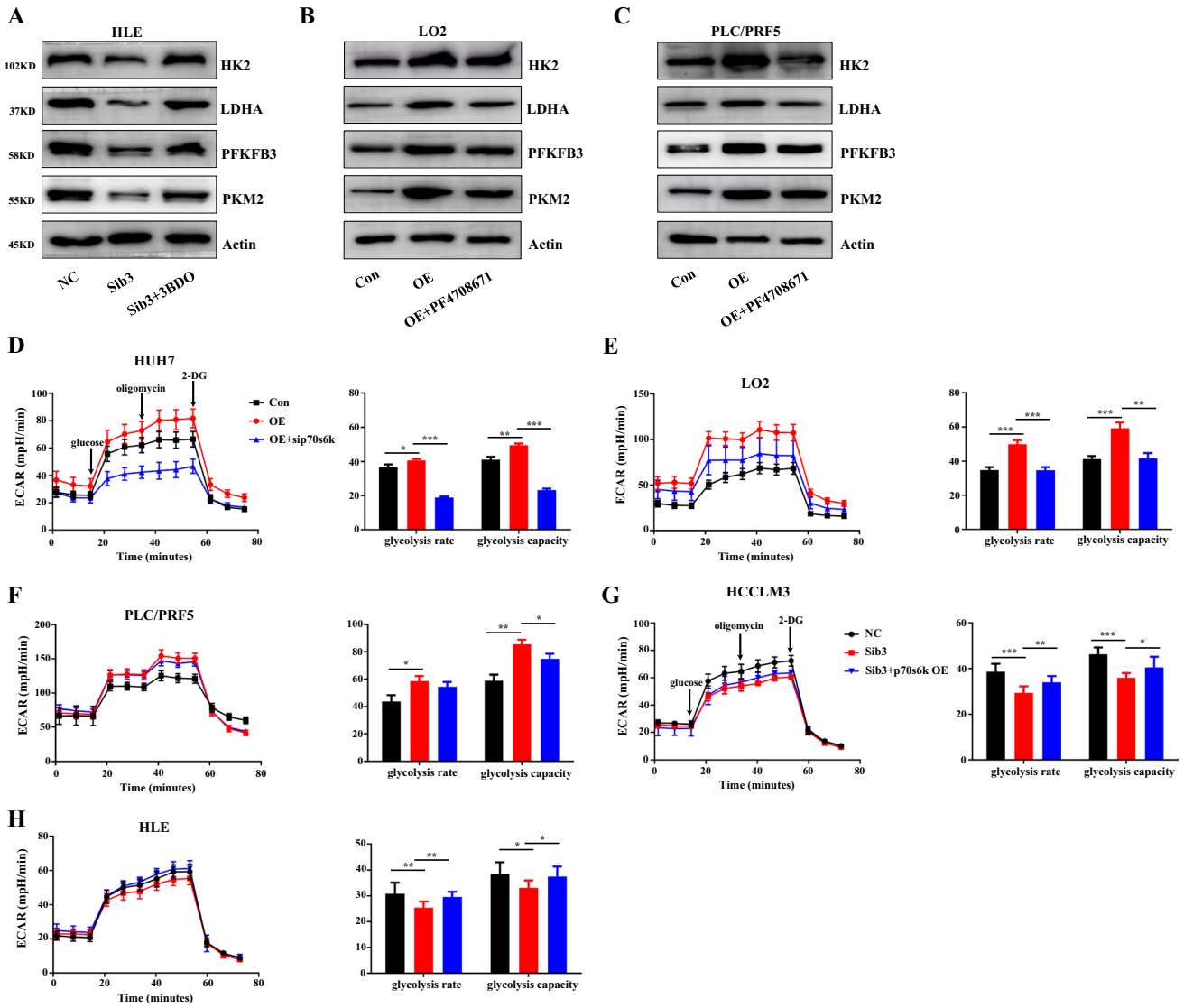

Fig. 5 B3galt5 promotes glycolysis by regulating the mTOR /p70s6k pathway. (**A**) Western blotting analysis of key glycolytic enzymes in HLE cells expressing control siRNA or b3galt5 siRNA treated with the p70s6k activator 3BDO. (**B**, **C**) Western blotting analysis of key glycolytic enzymes in b3galt5-overexpressing HCC cell lines treated with the p70s6k inhibitor PF4708671. (**D**–**F**) Analysis of ECAR in b3galt5-overexpressing HCC cell lines treated with p70s6k siRNA using the Seahorse XFe 96 Analyzer. (**G**, **H**) Analysis of ECAR in HCC cell lines expressing b3galt5 siRNA transfected with p70s6k overexpression lentivirus using the Seahorse XFe 96 Analyzer. $*p<0.05$, $**p<0.01$, $***p<0.001$

p-mTOR, while overexpression of b3galt5 enhanced their glycosylation modification (Fig. 6A). In the immunofluorescence assay, we confirmed a high fluorescence intensity of p-mTOR after b3galt5 overexpression, accompanied by the high fluorescence intensity of RCA-lectin, indicating the presence of galactose in p-mTOR (Fig. 6B). In contrast, b3galt5 knockdown correspondingly suppressed the fluorescence intensity (Fig. 6C).

B3galt5 is involved in both N-linked and O-linked glycosylation. PNGase F is an enzyme that hydrolyses the N-linked oligosaccharides [31]. O-glycosidase is an enzyme that catalyzes the removal of *core* 1 and *core* 3 O-linked disaccharides from glycoproteins, which is also known as Endo-α-*N*-acetylgalactosaminidase [32]. To further confirm the glycosylation of mTOR, we treated LO2 and PLC/PRF5 cells with PNGase F and O-glycosidase. Interestingly, the molecular weight of mTOR was significantly smaller upon O-glycosidase treatment, which increased its electrophoretic mobility (Fig. 7A). However, no changes in molecular weight or electrophoretic mobility of mTOR were observed after PNGase F treatment (Fig. 7B). Then, we examined whether b3galt5 mediated the glycosylation of mTOR. For this purpose, we treated HCC cells with O-glycosidase. The results indicated that the ratio of glycosylated mTOR decreased from 0.53 ± 0.28 to 0.30 ± 0.15 after b3galt5 silence in HCCLM3 cells, while the ratio increased from 0.64 ± 0.17 to 1.39 ± 0.20 in PLC/PRF5 cells after b3galt5 overexpressing (Fig. 7C, D). So the change of glycosylated mTOR was in line with the total mTOR. In addition, benzyl-α-GalNAc, an O-linked glycosylation inhibitor, led to the decreased expression of phosphorylated mTOR in HCCLM3 and LO2 cells (Fig. 7E, F).

Above all, these findings suggested that b3galt5 O-glycosylated and activated the mTOR pathway in HCC cells.

Discussion

Here, we reported that b3galt5 might be a driving factor in the development of HCC by potentiating glycolysis. We first identified that b3galt5 expression was highly elevated in HCC and positively associated with a poor prognosis. Then, we demonstrated that b3galt5 deficiency inhibited cell proliferation and hepatocarcinogenesis in vitro and in vivo. Mechanistically, we confirmed that b3galt5 played a tumorigenic role by promoting glycolysis in an mTOR O-glycosylation-dependent manner. Moreover, b3galt5 deficiency led to an impaired glycolytic phenotype, as indicated by decreased expression of key glycolytic enzymes and the glycolysis rate, further supporting the critical role of b3galt5 in HCC glucose metabolism.

The mTOR and HIF-α pathways are canonical pathways that regulate glycolysis [19]. mTOR inhibition was also reported to retarded the DEN-induced liver cancer model by down-regulating glycolysis capacity [33]. For example, farnesyl-diphosphate farnesyltransferase 1 downregulates glycolysis in colon cancer by inactivating the mTOR pathway [17]. Active mTORC1 directly increases glucose flux when the pentose phosphate pathway backs up into glycolysis, thereby circumventing a glycolysis block and ensuring adequate ATP and biomass production [34]. In our present study, we found that b3galt5 promotes aerobic glycolysis in hepatocellular carcinoma. This observation prompted us to further explore whether b3galt5 promoted aerobic glycolysis by regulating the mTOR pathway. We observed that depletion or silencing of b3galt5 in cells inhibited mTOR activation (Fig. 4). Surprisingly, total mTOR and p70s6k levels were also decreased. However, we could not rule out that the mTOR and p70s6k transcript levels were changed. Additional studies are needed to investigate whether b3galt5 regulates mTOR translation or affects their protein stability. Consistently, the impaired glycolytic phenotype caused by b3galt5 knockdown was partially rescued by activation or overexpression of p70s6k (Fig. 5G, H), while the activated glycolytic phenotype induced by b3galt5 overexpression could be partially reversed by inhibition or knockdown of p70s6k (Fig. 5D–F), which supported our hypothesis. Therefore, promotion of glycolysis through mTOR activation by b3galt5 might represent one mechanism for hepatocellular carcinoma to facilitate cell survival.

Altered glycosylation modification can markedly affect the functions of proteins, including interactions and signal transduction [35]. For instance, glycosylation of PD-L1 stabilizes its structure and thus participates in the interaction between PD-L1 and PD-1 [36]. Also the FUT8 mediated glycosylation on B7-H3 also affected its stability [37]. Considering that b3galt5 was involved in both N-linked and O-linked glycosylation, we further explored the underlying mechanisms of mTOR activation. To this end, we used RCA-lectin to confirm that b3galt5 participated in the glycosylation modification of mTOR. Then, we examined the expression of mTOR using the PNGase F and O-glycosidase. Our data demonstrated that O-glycosidase rather than PNGase F obviously reduced the molecular weight of mTOR. The ratio of glycosylated mTOR was increased when b3galt5 was overexpressed. Interestingly, benzy-α-GalNAc, an inhibitor of O-glycosylation [38], also significantly downregulated the phosphorylated mTOR expression. Based on these results, we hypothesized that O-linked glycosylation of mTOR influenced its activation and stability. To date, little is known about the glycosylation and functions of mTOR. Only a few articles have confirmed that O-GlcNAcylation of mTOR activated the mTOR [39]. O-GlcNAcylation is the covalent linkage of GlcNAc glycans to serine and threonine residues

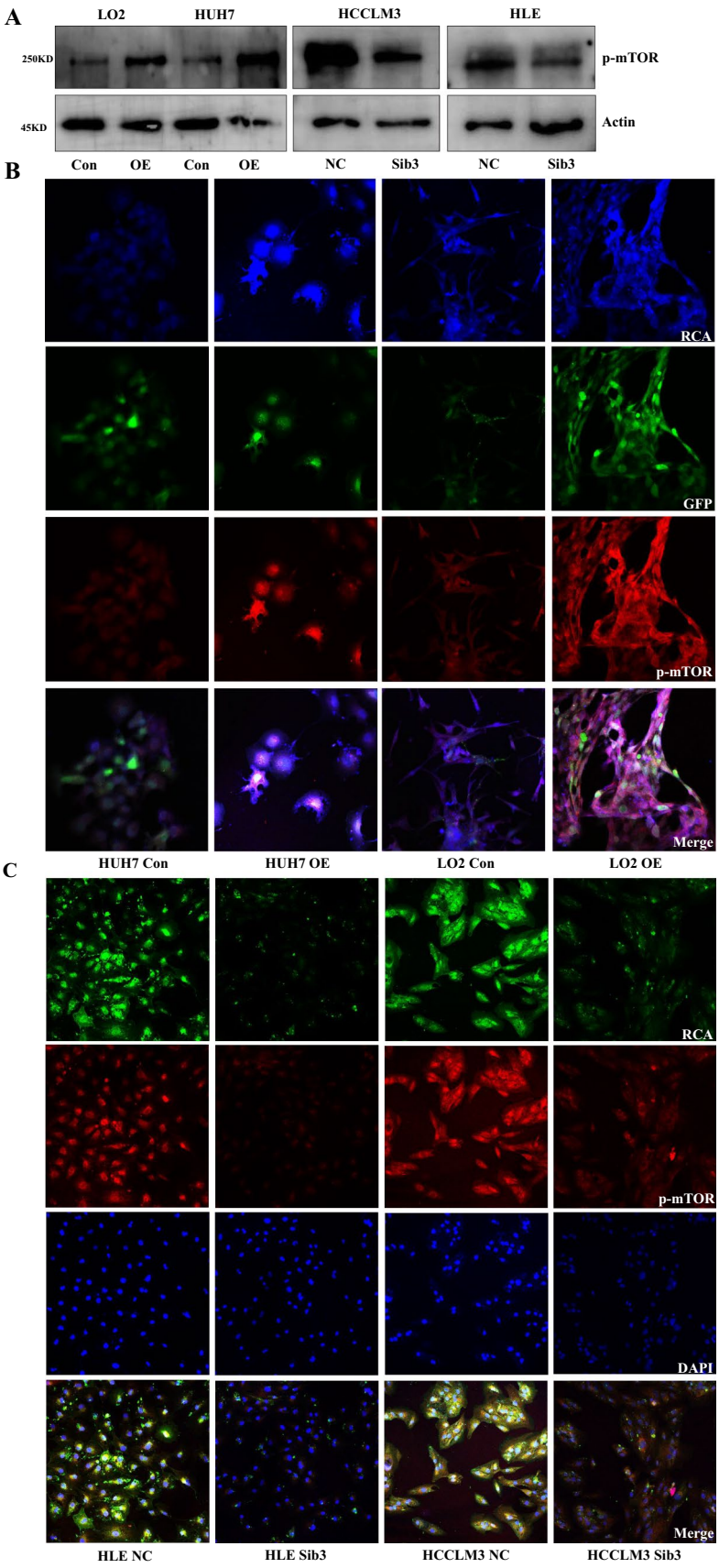

Fig. 6 B3galt5 activates mTOR through galactosylation. (**A**) The effect of b3galt5 on galactosylation of p-mTOR by the RCA-I/II antibody IP assay. HCCLM3 and HLE cells transfected with b3galt5 siRNA or NC siRNA were lysed with NP40 and incubated with RCA-I/II antibody and protein A/G agarose beads overnight. LO2 and HUH7 cells overexpressing b3galt5 were lysed with NP40 and incubated with RCA-I/II antibody and protein A/G agarose beads overnight. (**B**) HUH7 and LO2 cells were transduced with control lentivirus or lentivirus for GFP-b3galt5 expression. Representative images of RCA-I/II (blue) and p-mTOR immunostaining (red) in b3galt5-overexpressing HCC cells. Magnification, × 200. (**C**) HLE and HCCLM3 cells were transfected with 50 nM control siRNA or b3galt5-specific siRNAs. Representative images of RCA-I/II (green), p-mTOR immunostaining (red), and DAPI (blue) in b3galt5 knockdown HCC cells. Magnification, × 200

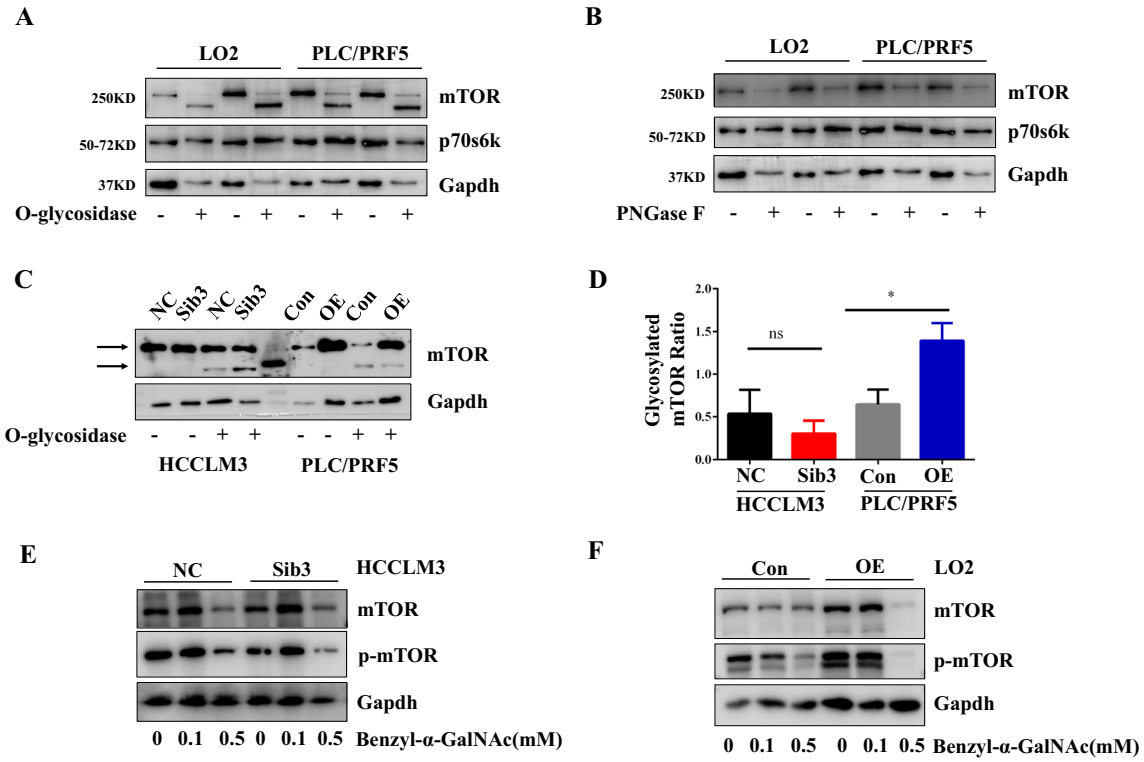

Fig. 7 O-linked glycosylation on mTOR influences its phosphorylation. (**A**, **B**) The cell lysates were treated with PNGase F and O-glycosidase and analyzed by western blotting. The cell lysis was loaded twice. (**C**) Western blotting analysis of mTOR in HCCLM3 cells with b3galt5 knockdown or control siRNA or in PLC/PRF5 cells with b3galt5 overexpression or control vector treated by O-glycosidase. The non-glycosylated mTOR was displayed in the lower arrows, the glycosylated mTOR was displayed in the upper arrows. (**D**) The ratio of glycosylated mTOR of HCCLM3 and PLC/PRF5 were analyzed by Image J, HCCLM3 = 3, PLC/PRF5 = 4. Data are represented as mean ± S.E.M. (**E**, **F**) Western blotting analysis of p-mTOR in cells treated with the O-glycosylation inhibitor benzyl-α-GalNac with increasing concentrations (0.1 and 0.5 mM for 24 h)

of protein substrates, which is catalyzed by O-linked N-acetylglucosamine transferase (OGT) [40]. Thus, our study is the first attempt to explore b3galt5-mediated mTOR O-glycosylation and its effect on mTOR activation. More evidence is needed to further confirm how b3galt5 modifies the O-glycosylation of mTOR. Further experiments like isotope labeled glycan and glycoprotein spectrum analysis may help to identify the specific chains of mTOR. O-linked glycosylation was reported to influence the function of protein, for instances, intracellular O-linked glycosylation directly regulates cardiomyocyte L-type Ca2 + channel activity [41]. O-linked glycosylation on CaMKII enhances CaMKII activity autonomously [42], O-linked glycosylation of A20 also enhances the inhibition of NF-κb activation [43]. Moreover, how O-glycosylation activates mTOR needs to be further explored.

Emerging evidence suggests that glycosylation plays an important role in cancer stemness. Cancer stem cell markers are mainly glycoproteins, such as CD44, CD133, and CD24 [44]. α-1,3-Mannosyltransferase, which is involved in early N-glycan synthesis, promotes breast cancer stemness by inducing glycosylation of TGF-β receptor II [45]. β1,4-N-Acetylgalactosaminyltransferase III regulates stemness by inducing the expression of the colon cancer stem cell markers OCT4 and NANOG [46]. B3galt5 has been reported to promote breast cancer progression by enhancing cancer stemness [9]. In this study, we found that the regulatory role of b3galt5 in HCC involved another mechanism, that is, promoting mTOR glycosylation to enhance glycolysis. It should be noted that we cannot exclude whether b3galt5 may also contribute to the regulation of liver cancer stemness. Studies have indicated that metabolic reprogramming can regulate cancer cell stemness [47]. For instance, the glycolysis gatekeeper PDK1 reprogrammed breast cancer cell stemness under hypoxic conditions [48]. In addition, the mTOR pathway was reported to be closely related to the maintenance of cancer stem cells [49, 50]. Inhibition of the mTOR pathway in breast cancer stem-like cells significantly suppressed not only colony-formation ability in vitro but also tumorigenicity in vivo [51]. Positive expression of p-mTOR was positively associated with positive expression of the liver cancer stem cell markers CD133, CD90, and EpCAM [52]. In addition, mTOR direct down-stream p70s6k also regulates the stemness and

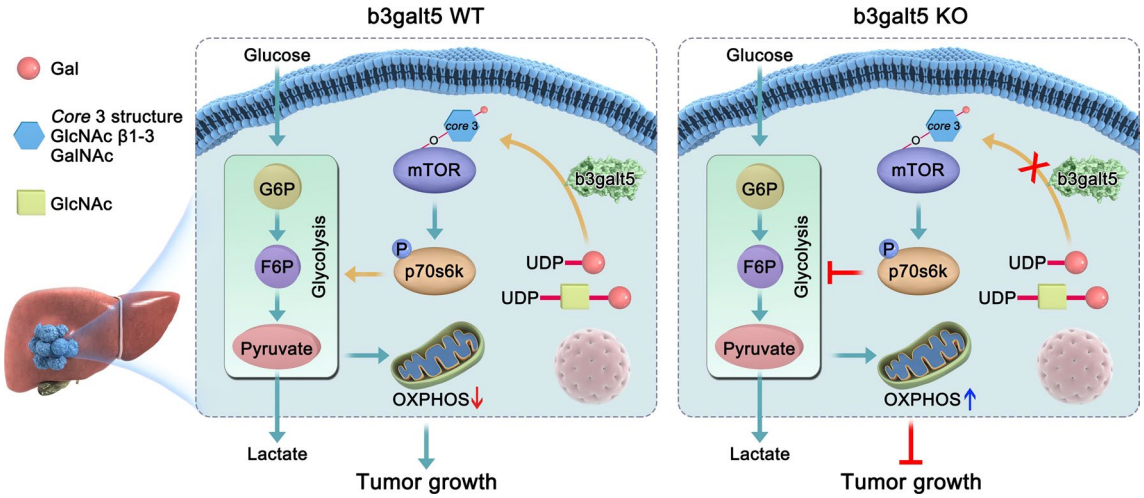

Fig. 8 Schematic diagram of the b3galt5-mediated effects on hepatocellular carcinoma. Elevated expression of b3galt5 in HCC cells promoted mTOR glycosylation, which contributed to enhanced aerobic glycolysis. Activation of mTOR promotes HCC cell proliferation and survival by diverting glucose metabolism from OXPHOS to glycolysis. On the other hand, depletion of b3galt5 eliminated glycosylation to inhibit mTOR activation, which promoted glucose metabolism into OXPHOS, thus inhibiting HCC cell survival

metastatic properties of ovarian cancer cells, knocking down p70s6k leading to a marked reduction in cancer stem cell proliferation and expansion [53]. P19 stem cells pluripotency was also relied on PI3K-AKT-mTOR-p70s6k pathway activation [54]. Therefore, it is necessary to further illustrate the role of b3galt5 in liver cancer stemness.

Conclusions

Our findings unveiled a novel function of b3galt5 in regulating glycolysis in hepatocellular carcinoma. B3galt5 promoted O-linked glycosylation modification of mTOR and thus activated its downstream signaling, resulting in metabolic reprogramming from OXPHOS to glycolysis (Fig. 8). This study provides a new biomarker and potential target for the diagnosis and treatment of liver cancer.

Supplementary Information The online version contains supplementary material available at https://doi.org/10.1007/s00018-022-04601-x.

Acknowledgements We are grateful to Prof. Jinhan He at the Department of Pharmacy, West China Hospital of Sichuan University, for sharing the b3galt5$^{-/-}$ mice.

Author contributions PHM and HWD designed and supervised the project; ZXL, LH, LQ, WHD, LYL, and HYC performed the animal and cell experiments; WHD and ZXL performed the glycosidase experiment, ZRJ analyzed the GEO database; and ZXL, LH, RLL and HWD wrote and edited the manuscript. All of the coauthors reviewed the manuscript.

Funding This work was supported by the National Natural Science Foundation of China (81972745 and 81703072), the Ten Thousand Plan Youth Talent Support Program of Zhejiang Province (ZJWR0108009), and the Zhejiang Medical Innovative Discipline Construction Project-2016.

Availability of data and materials All data generated during this study are included in this published article and its supplementary files.

Declarations

Competing interests The authors declare no conflicts of interest.

Ethics approval and consent to participate This study was approved by the Ethics Committee of Zhejiang University. All the animal experiments performed in this study were approved by the Institutional Animal Care and Use Committee of Zhejiang University.

Consent for publication All authors consent this manuscript to be published.

References

1. Bennett EP, Mandel U, Clausen H, Gerken TA, Fritz TA, Tabak LA (2012) Control of mucin-type O-glycosylation: a classification of the polypeptide GalNAc-transferase gene family. Glycobiology 22(6):736–756
2. Cherepanova N, Shrimal S, Gilmore R (2016) N-linked glycosylation and homeostasis of the endoplasmic reticulum. Curr Opin Cell Biol 41:57–65
3. Zhang S, Cao X, Gao Q, Liu Y (2017) Protein glycosylation in viral hepatitis-related HCC: characterization of heterogeneity, biological roles, and clinical implications. Cancer Lett 406:64–70
4. Chikhaliwala P, Rai R, Chandra S (2019) Simultaneous voltammetric immunodetection of alpha-fetoprotein and glypican-3 using a glassy carbon electrode modified with magnetite-conjugated dendrimers. Mikrochim Acta 186:255
5. Eichler J (2019) Protein glycosylation. Curr Biol. 29(7):229–231

6. Salvini R, Bardoni A, Valli M, Trinchera M (2001) beta 1,3-galactosyltransferase beta 3Gal-T5 acts on the GlcNAcbeta 1–>3Galbeta 1–>4GlcNAcbeta 1–>R sugar chains of carcinoembryonic antigen and other N-linked glycoproteins and is down-regulated in colon adenocarcinomas. J Biol Chem 276:3564–3573
7. Zhou D, Berger EG, Hennet T (1999) Molecular cloning of a human UDP-galactose:GlcNAcbeta1,3GalNAc beta1, 3 galactosyltransferase gene encoding an O-linked core3-elongation enzyme. Eur J Biochem 263:571–576
8. Liao YM, Wang YH, Hung JT et al (2021) High B3GALT5 expression confers poor clinical outcome and contributes to tumor progression and metastasis in breast cancer. Breast Cancer Res 23:5
9. Chuang PK, Hsiao M, Hsu TL et al (2019) Signaling pathway of globo-series glycosphingolipids and β1,3-galactosyltransferase V (β3GalT5) in breast cancer. Proc Natl Acad Sci U S A 116(9):3518–3523
10. Engle DD, Tiriac H, Rivera KD et al (2019) The glycan CA19-9 promotes pancreatitis and pancreatic cancer in mice. Science 364(6446):1156–1162
11. Seko A, Kataoka F, Aoki D et al (2009) Beta 1,3-galactosyltransferases-4/5 are novel tumor markers for gynecological cancers. Tumour Biol 30:43–50
12. Estes C, Anstee QM, Arias-Loste MT et al (2018) Modeling NAFLD disease burden in China, France, Germany, Italy, Japan, Spain, United Kingdom, and United States for the period 2016–2030. J Hepatol 69(4):896–904
13. Beyoğlu D, Imbeaud S, Maurhofer O et al (2013) Tissue metabolomics of hepatocellular carcinoma: tumor energy metabolism and the role of transcriptomic classification. Hepatology 58:229–238
14. Ma R, Zhang W, Tang K et al (2013) Switch of glycolysis to gluconeogenesis by dexamethasone for treatment of hepatocarcinoma. Nat Commun 4:2508
15. Kowalik MA, Guzzo G, Morandi A et al (2016) Metabolic reprogramming identifies the most aggressive lesions at early phases of hepatic carcinogenesis. Oncotarget 7(22):32375–32393
16. Ling S, Shan Q, Zhan Q et al (2020) USP22 promotes hypoxia-induced hepatocellular carcinoma stemness by a HIF1α/USP22 positive feedback loop upon TP53 inactivation. Gut 69:1322–1334
17. Weng ML, Chen WK, Chen XY et al (2020) Fasting inhibits aerobic glycolysis and proliferation in colorectal cancer via the Fdft1-mediated AKT/mTOR/HIF1α pathway suppression. Nat Commun 11:1869
18. Wu H, Pan L, Gao C et al (2019) Quercetin inhibits the proliferation of glycolysis-addicted HCC Cells by reducing hexokinase 2 and Akt-mTOR pathway. Molecules 24:2
19. Cheng SC, Quintin J, Cramer RA et al (2014) mTOR- and HIF-1α-mediated aerobic glycolysis as metabolic basis for trained immunity. Science 345(6204):1250684
20. Kuo HH, Lin RJ, Hung JT et al (2017) High expression FUT1 and B3GALT5 is an independent predictor of postoperative recurrence and survival in hepatocellular carcinoma. Sci Rep 7(1):10750
21. Kang X, Wang N, Pei C et al (2012) Glycan-related gene expression signatures in human metastatic hepatocellular carcinoma cells. Exp Ther Med 3:415–422
22. Chung TW, Kim SJ, Choi HJ et al (2014) Hepatitis B virus X protein specially regulates the sialyl Lewis a synthesis among glycosylation events for metastasis. Mol Cancer 13:222
23. Dorsch MA, de Yaniz MG, Fiorani F et al (2019) A descriptive study of lectin histochemistry of the placenta in cattle following inoculation of Neospora caninum. J Comp Pathol 166:45–53. https://doi.org/10.1016/j.jcpa.2018.10.172
24. Jang JS, Wang X, Vedell PT, Wen J, Zhang J, Ellison DW, Evans JM, Johnson SH, Yang P, Sukov WR et al (2016) Custom gene capture and next-generation sequencing to resolve discordant ALK status by FISH and IHC in lung adenocarcinoma. J Thorac Oncol 11:1891–1900
25. Balsa E, Soustek MS, Thomas A et al (2019) ER and nutrient stress promote assembly of respiratory chain supercomplexes through the PERK-eIF2α axis. Mol Cell 74:877–90.e6
26. Saada A, Vogel RO, Hoefs SJ et al (2009) Mutations in NDUFAF3 (C3ORF60), encoding an NDUFAF4 (C6ORF66)-interacting complex I assembly protein, cause fatal neonatal mitochondrial disease. Am J Hum Genet 84:718–727
27. Bourens M, Barrientos A (2017) A CMC1-knockout reveals translation-independent control of human mitochondrial complex IV biogenesis. EMBO Rep 18:477–494
28. Van Vranken JG, Bricker DK, Dephoure N et al (2014) SDHAF4 promotes mitochondrial succinate dehydrogenase activity and prevents neurodegeneration. Cell Metab 20:241–252
29. Iansante V, Choy PM, Fung SW et al (2015) PARP14 promotes the Warburg effect in hepatocellular carcinoma by inhibiting JNK1-dependent PKM2 phosphorylation and activation. Nat Commun 6:7882
30. Kato T, Wang Y, Yamaguchi K et al (2001) Overexpression of lysosomal-type sialidase leads to suppression of metastasis associated with reversion of malignant phenotype in murine B16 melanoma cells. Int J Cancer 92(6):797–804
31. Li JV, Ng CA, Cheng D, Zhou Z, Yao M, Guo Y, Yu ZY, Ramaswamy Y, Ju LA, Kuchel PW, Feneley MP, Fatkin D, Cox CD (2021) Modified N-linked glycosylation status predicts trafficking defective human Piezo1 channel mutations. Commun Biol 4:1038. https://doi.org/10.1038/s42003-021-02528-w
32. Yang S, Onigman P, Wu WW, Sjogren J, Nyhlen H, Shen RF, Cipollo J (2018) Deciphering protein O-glycosylation: solid-phase chemoenzymatic cleavage and enrichment. Anal Chem 90:8261–8269. https://doi.org/10.1021/acs.analchem.8b01834
33. Yao L, Xuan Y, Zhang H, Yang B, Ma X, Wang T, Meng T, Sun W, Wei H, Ma X et al (2021) Reciprocal REGγ-mTORC1 regulation promotes glycolytic metabolism in hepatocellular carcinoma. Oncogene 40:677–692
34. Pusapati RV, Daemen A, Wilson C et al (2016) mTORC1-dependent metabolic reprogramming underlies escape from glycolysis addiction in cancer cells. Cancer Cell 29(4):548–562
35. Spiro RG (2002) Protein glycosylation: nature, distribution, enzymatic formation, and disease implications of glycopeptide bonds. Glycobiology 12:43R-56R
36. Lee HH, Wang YN, Xia W et al (2019) Removal of N-linked glycosylation enhances PD-L1 detection and predicts anti-PD-1/PD-L1 therapeutic efficacy. Cancer Cell 36:168–78.e4
37. Huang Y, Zhang HL, Li ZL, Du T, Chen YH, Wang Y, Ni HH, Zhang KM, Mai J, Hu BX, Huang JH, Zhou LH, Yang D, Peng XD, Feng GK, Tang J, Zhu XF, Deng R (2021) FUT8-mediated aberrant N-glycosylation of B7H3 suppresses the immune response in triple-negative breast cancer. Nat Commun 12:2672. https://doi.org/10.1038/s41467-021-22618-x
38. Kalra AV, Campbell RB (2007) Mucin impedes cytotoxic effect of 5-FU against growth of human pancreatic cancer cells: overcoming cellular barriers for therapeutic gain. Br J Cancer 97:910–918. https://doi.org/10.1038/sj.bjc.6603972
39. Yin S, Liu L, Gan W (2021) The roles of post-translational modifications on mTOR signaling. Int J Mol Sci 22:2
40. Pyo KE, Kim CR, Lee M, Kim JS, Kim KI, Baek SH (2018) ULK1 O-GlcN acylation is crucial for activating VPS34 via ATG14L during autophagy initiation. Cell Rep 25:2878-2890.e4. https://doi.org/10.1016/j.celrep.2018.11.042
41. Ednie AR, Bennett ES (2020) Intracellular O-linked glycosylation directly regulates cardiomyocyte L-type Ca(2+) channel activity and excitation-contraction coupling. Basic Res Cardiol 115:59. https://doi.org/10.1007/s00395-020-00820-0

42. Wang C, Li Y, Yan S, Wang H, Shao X, Xiao M, Yang B, Qin G, Kong R, Chen R, Zhang N (2020) Interactome analysis reveals that lncRNA HULC promotes aerobic glycolysis through LDHA and PKM2. Nat Commun 11:3162. https://doi.org/10.1038/s41467-020-16966-3
43. Yao D, Xu L, Xu O, Li R, Chen M, Shen H, Zhu H, Zhang F, Yao D, Chen YF, Oparil S, Zhang Z, Gong K (2018) O-Linked β-N-acetylglucosamine modification of A20 enhances the inhibition of NF-κB (nuclear factor-κB) activation and elicits vascular protection after acute endoluminal arterial injury. Arterioscler Thromb Vasc Biol 38:1309–1320. https://doi.org/10.1161/ATVBAHA.117.310468
44. Barkeer S, Chugh S, Batra SK, Ponnusamy MP (2018) Glycosylation of cancer stem cells: function in stemness, tumorigenesis, and metastasis. Neoplasia 20:813–825
45. Sun X, He Z, Guo L et al (2021) ALG3 contributes to stemness and radioresistance through regulating glycosylation of TGF-β receptor II in breast cancer. J Exp Clin Cancer Res 40:149
46. Che MI, Huang J, Hung JS et al (2014) β1, 4-N-acetylgalactosaminyltransferase III modulates cancer stemness through EGFR signaling pathway in colon cancer cells. Oncotarget 5:3673–3684
47. Menendez JA (2015) Metabolic control of cancer cell stemness: lessons from iPS cells. Cell Cycle 14:3801–3811
48. Peng F, Wang JH, Fan WJ et al (2018) Glycolysis gatekeeper PDK1 reprograms breast cancer stem cells under hypoxia. Oncogene 37:1062–1074
49. Honjo S, Ajani JA, Scott AW et al (2014) Metformin sensitizes chemotherapy by targeting cancer stem cells and the mTOR pathway in esophageal cancer. Int J Oncol 45:567–574
50. Mohammed A, Janakiram NB, Brewer M et al (2013) Antidiabetic drug metformin prevents progression of pancreatic cancer by targeting in part cancer stem cells and mTOR signaling. Transl Oncol 6:649–659
51. Zhou J, Wulfkuhle J, Zhang H et al (2007) Activation of the PTEN/mTOR/STAT3 pathway in breast cancer stem-like cells is required for viability and maintenance. Proc Natl Acad Sci U S A 104:16158–16163
52. Su R, Nan H, Guo H et al (2016) Associations of components of PTEN/AKT/mTOR pathway with cancer stem cell markers and prognostic value of these biomarkers in hepatocellular carcinoma. Hepatol Res 46:1380–1391
53. Ma J, Kala S, Yung S, Chan TM, Cao Y, Jiang Y, Liu X, Giorgio S, Peng L (2018) Blocking stemness and metastatic properties of ovarian cancer cells by targeting p70s6k with dendrimer nanovector-based siRNA delivery. Mol Ther 26:70–83
54. Magalhães-Novais S, Bermejo-Millo JC, Loureiro R, Mesquita KA, Domingues MR, Maciel E, Melo T, Baldeiras I, Erickson JR, Holy J et al (2020) Cell quality control mechanisms maintain stemness and differentiation potential of P19 embryonic carcinoma cells. Autophagy 16:313–333